IEEE Access
Multidisciplinary | Rapid Review | Open Access Journal

Received October 6, 2020, accepted November 3, 2020, date of publication November 23, 2020, date of current version December 1, 2020.

Digital Object Identifier 10.1109/ACCESS.2020.3038058

T-A Formulation for the Design and AC Loss Calculation of a Superconducting Generator for a 10 MW Wind Turbine

CARLOS ROBERTO VARGAS-LLANOS[1], SEBASTIAN LENGSFELD[2], AND FRANCESCO GRILLI[1]
[1]Institute for Technical Physics, Karlsruhe Institute of Technology (KIT), 76131 Karlsruhe, Germany
[2]Fraunhofer Institute for Energy Economics and Energy System Technology, 34119 Kassel, Germany

Corresponding author: Francesco Grilli (francesco.grilli@kit.edu)

The underlying work of this article was funded by the German Federal Ministry for Economic Affairs and Energy (project name ''SupraGenSys'', funding reference number 03EE3010A and 03EE3010D). The responsibility for the content of this article lies with the authors and does not necessarily reflect the opinion of the SupraGenSys project consortium. The authors acknowledge support by the KIT-Publication Fund of the Karlsruhe Institute of Technology.

ABSTRACT The current capacity of high-temperature superconductors (HTS) has encouraged several applications of these materials in electric power systems. These applications in electrical machines represent a promising solution for more compact and efficient designs. Despite no measurable resistance in the superconducting state, HTS could experience losses under time changing transport current or magnetic field. Therefore, loss estimation is a key input for the design. Maxwell's equations in the T-A formulation form can be used to model and estimate losses in the superconducting tapes of an electrical machine. This formulation requires the current as a function of time in each superconducting tape as an input. A methodology to calculate this current distribution is presented in this article. The procedure introduces a previous step in the building model process and allows a better connection of the machine design with the estimation of losses in the superconductor in order to get a more efficient machine. The approach is applied to a 10 MW superconducting generator, where over one thousand tapes cross-sections are modelled in 2D. The superconductor's non-linear behaviour and critical current density anisotropy are considered. Losses are estimated for different designs and a sensitivity analysis is presented for different temperatures and frequencies, in addition to other alternatives to reduce losses.

INDEX TERMS AC losses, superconducting generator, high-temperature superconductors, T-A formulation.

I. INTRODUCTION

The electrical properties of high-temperature superconductors (HTS) can provide good solutions to several problems in electric power systems. Their zero resistance could lead to a reduction in energy loss and their high current capacity into a size and weight reduction in power components and machinery [1]. HTS attributes have encouraged research in several applications like electrical machines [2], [3]; energy storage [4] and transmission [5]; and fault current limiters [1], [6].

The increasing worldwide energy consumption and renewable generation have driven strong research on superconducting generators for wind turbine applications, where HTS could increase power density towards better multi-megawatt solutions [7]–[11]. Even with no measurable resistance, HTS materials experience energy dissipation when they are exposed to changes in current or magnetic field [12]. As a consequence, most of these applications involve so far only HTS tapes in the rotor/field winding, which carries DC-current. In stator coils, they could experience higher losses. Moreover, they have to operate under cryogenic temperatures to keep the superconducting properties. Under this condition, the cooling efficiency has a great impact on the refrigeration power required to handle energy dissipation. Therefore, loss estimation becomes a key factor in the design of the machine, strongly influencing the practical and economical realization of such applications [2], [13].

Analytical solutions have been developed to estimate losses in single tapes [14], [15] and infinite stacks of superconducting tapes [16]–[18], under transport current or externally applied magnetic field. However, these expressions do not fully represent the real behaviour of the losses in superconducting coils located in the stator of an electrical machine,

The associate editor coordinating the review of this manuscript and approving it for publication was Lei Chen.

This work is licensed under a Creative Commons Attribution-NonCommercial-NoDerivatives 4.0 License.
For more information, see https://creativecommons.org/licenses/by-nc-nd/4.0/

since they will be exposed to a rotating magnetic field and AC transport current. As a consequence, a finite element method application is required based on Maxwell's equations and considering the superconducting non-linear behaviour. Not only can this model estimate losses in the superconducting coils, but it can also improve the overall machine towards a better design solution.

This publication is based on a design study of a superconducting generator for a wind turbine application, which uses permanent magnets in the rotor and superconducting coils in the stator. Electromagnetic behaviour and loss estimation are assessed by means of T-A formulation of Maxwell's equations, implemented in the commercial software Comsol Multiphysics. The current as a function of time in each superconducting tape is determined by following a proposed methodology, which is guided by the building model process. Symmetries are used to enable simulating the machine's cross-sections by considering every HTS tape and its non-linear behaviour. This approach is applied to three possible designs, each one of them with different stator configurations. Electromagnetic improvements are proposed in this publication to enhance energy dissipation behaviour in the superconducting coils. In this work, we first present the proposed modelling approach in section II, followed by a description of the three designs under study and its material's basic characteristics in section III. Finally, electromagnetic behaviours and estimation of losses are analyzed in section IV, where sensitivity studies are conducted over different speeds/frequencies and average operating temperatures of the coils. All the results and findings are summarized in the conclusion and a validation of the T-A formulation against measurements is presented in the Appendix.

II. MODELLING APPROACH

The models in this publication are a 2D representation of the cross-section of an electrical machine. This means that the end-effects (winding heads) in the machine are not considered. We estimate the total losses by multiplying the 2D results by the effective length of the electrical machine.

In this work, the T-A formulation is used to study the electromagnetic behaviour and estimate the losses in the superconducting tapes. This formulation has already been used in previous studies to model cross-sections of superconducting electrical machines with a few hundred tapes [19]–[22]. This methodology requires the current as a function of time in each superconducting tape. For problems involving electrical machines, this input is traditionally computed with an external software/model. Therefore, a direct connection of the estimation of losses with the basic machine design is not easy to achieve. Here, we follow an approach that estimates the required current distribution as a step to build the numerical model. This allows us to estimate losses, calculate torque and propose design improvements with the same program. Since the cross-sections of the electrical machines under study involve thousands of superconducting tapes, some symmetries are considered to reduce the size of the problem.

A. T-A FORMULATION

This formulation of Maxwell's equations was introduced in [23] and it has been used for modelling several superconducting devices [24]–[26]. In this approach, the magnetic vector potential $\mathbf{A}$ is computed in the entire geometry as:

$$\nabla \times (\frac{1}{\mu} \nabla \times \mathbf{A}) = \mathbf{J} \tag{1}$$

where $\mathbf{J}$ is the current density, μ is the permeability of the material and $\mathbf{A}$ is defined as $\mathbf{B} = \nabla \times \mathbf{A}$ ($\mathbf{B}$, magnetic flux density). $\mathbf{T}$, defined as $\mathbf{J} = \nabla \times \mathbf{T}$, is only computed in the superconducting domain as:

$$\nabla \times (\rho_{HTS} \nabla \times \mathbf{T}) = -\frac{\partial \mathbf{B}}{\partial t} \tag{2}$$

In this publication, an auxiliary cylindrical coordinate system is used to easily define permanent magnets properties as well as north and south directions. The resistivity of the superconducting material is modelled with a power-law **E-J** relation [27]:

$$\rho_{HTS} = \frac{E_c}{J_c(\mathbf{B})} \left| \frac{\mathbf{J}}{J_c(\mathbf{B})} \right|^{n-1} \tag{3}$$

In this expression, we assumed a critical electric field $E_c = 1 \times 10^{-4}\,\mathrm{V\,m^{-1}}$ and a value of $n = 25$. The critical current density as a function of magnetic flux density ($J_c(\mathbf{B})$) will be defined in the following section, where the superconducting tape used in the electrical machine design is described.

The T-A formulation is particularly useful for simulating rare earth barium copper oxide (REBCO) tapes. The high aspect ratio of these HTS tapes allows using a thin strip approximation, where the cross-section of the conductor is collapsed into a 1D object in a 2D model [23], [24]. This reduces the computation time. Following this approach, we can compute the current directly by integrating the current density in the tape cross-section (S, delimited by the path ∂S):

$$I = \iint_S \mathbf{J}\, dS = \iint_S \nabla \times \mathbf{T}\, dS = \oint_{\partial S} \mathbf{T}\, dl \tag{4}$$

The above mentioned integral can be further reduced by assuming a 1D element, which yields the following expression [25]:

$$I = (T_1 - T_2)\delta, \tag{5}$$

where δ is the thickness of the superconducting layer of the tape, T_1 and T_2 are the current potentials at the extremes of the layer. Hence, the current in the HTS tape is enforced by assigning appropriate values to T_1 and T_2.

The validation of this modelling technique is presented in appendix, where losses were estimated for a circular coil with sinusoidal transport current and compared with measurements from [28].

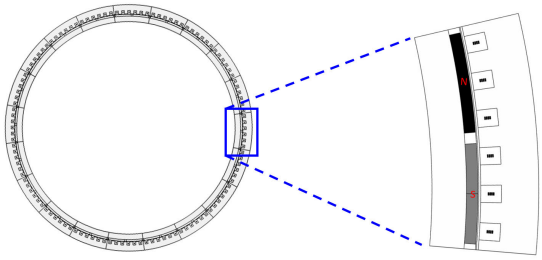

FIGURE 1. Zoom-in one pole pair of an electrical machine.

B. SYMMETRIES

The cross-sections of the 10 MW superconducting generators under analysis have several thousands of tapes, permanent magnets and magnetic materials with non-linear $\mathbf{B}-\mathbf{H}$ relation. Moreover, we model the resistivity of the HTS tapes by using the aforementioned $\mathbf{E}-\mathbf{J}$ power-law relation, where the critical current density depends on temperature and magnetic field amplitude and direction. The number of degrees of freedom (DOF) arising from modelling the whole cross-section of these electrical machines is very large. Therefore, the simulated models are reduced to one pole pair as it can be observed in Fig. 1, where the whole cross-section of a 20 pole pairs electrical machine is shown. A zoom in one pole pair is depicted in blue (north and south poles are in black and gray colors). Continuity periodic conditions are taken in the upper and lower boundaries of this pole pair. Hence the whole cross-section can be re-built in the post-processing through rotation of the computed solution.

C. MODELS

We propose an approach where the stator coils current distribution is computed in a basic model by connecting a load to the generator, taking into account the current in each HTS tape is needed as an input for the T-A formulation. Once we have the current distribution, the load is disconnected (resistive model) and superconducting coils details are added (superconducting model). As a consequence, we built one model to make design improvements and one to estimate losses in a single process. A brief description of the building model procedure is presented in Fig. 2. An additional superconducting model is considered in this section, which allows reducing the computation time by modelling only one coil group cross-section as HTS material.

- *Resistive model:* the geometry of the cross-section of the coils is typically homogenized when modelling conventional machines. Each coil cross-section is represented by a homogeneous block with approximately the same electromagnetic behaviour as a fully detailed cross-section [29]–[31]. Therefore, we develop first this simplified resistive model (without the superconducting material) based on this approach. Initially, a resistive load is connected to the model and current flows as a result of induced voltage in the coils. These induced currents are the necessary input for the T-A formulation. In the following step, we feed the induced current distribution into the same model, disconnect the load and adjust the amplitude to the nominal power of the machine if necessary.
  The induced currents, arising from the connected resistive load, can include several harmonics that can be analyzed by using Fourier Transform. However, we assume that the amplitude of the harmonics is too low to generate an important impact on the estimation of losses as they could be significantly reduced in this or previous stages of the design. Moreover, the main objective of our study is not related to harmonic content analysis or mitigation, but to electromagnetic modelling and loss estimation. Therefore, we only consider the fundamental signal.
  In this model, the torque density and the general electromagnetic behaviour can be analyzed. Since the computation time is within the range of minutes, several improvements and re-runs can be quickly done.
- *Superconducting model:* once we have the current distribution, we can import it into a model that considers the HTS material. We replace the homogenized coils cross-sections by detailed stacks of tapes, use the T-A formulation and impose the current distribution with (5). The electromagnetic behaviour and loss estimation can be directly analyzed in each HTS tape of the machine by using this model. However, the computation time is still too high (in the range of days) with conventional commercially available computers.
- *Model with only one coil group considered as HTS tapes:* as it will be shown in the following sections, the electromagnetic behaviour in each group of phase coils cross-section is very similar (shifted in time and/or space). As a consequence, we can model only one group of coils with details. This model allows us to estimate losses in all the superconducting tapes within a reasonable time (in the range of hours) with conventional commercially available computers.

III. MACHINE DESIGN AND MATERIALS

The electrical machine under study is a 10 MW synchronous superconducting generator, where the rotor is equipped with permanent magnets and the stator superconducting coils are made with REBCO tapes. We consider only the superconducting material is operating under cryogenic temperatures; trying to reduce the cooling power requirements and taking into account losses in the magnetic material can increase under low temperatures [32]. A brief description of the materials used in the model is presented in this section, as well as several alternative designs.

A. SUPERCONDUCTING TAPE

The stator coils are wound with a 4 mm HTS REBCO tape manufactured by SuperPower Inc, more detailed information about it can be found in [33]. This tape is modelled by considering only the superconducting layer surrounded by a homogeneous medium with a resistivity of 1 Ω m and

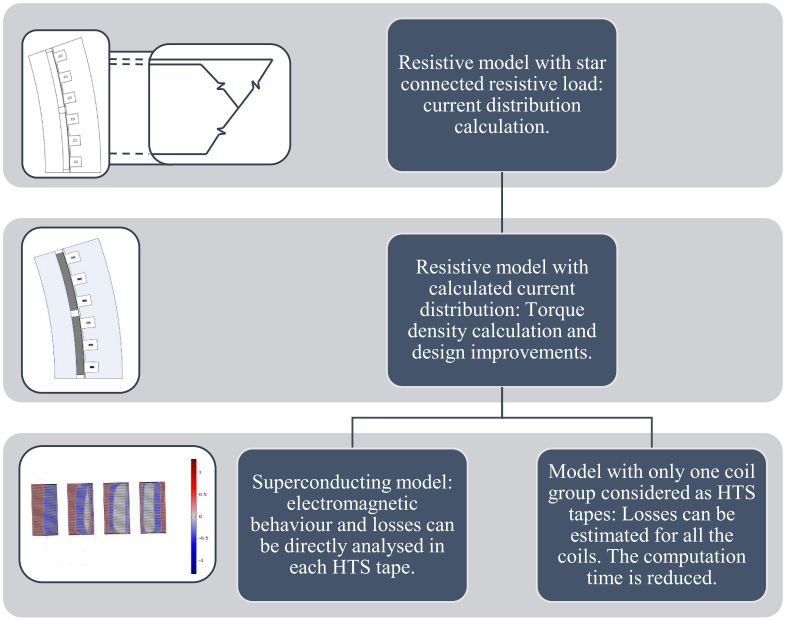

FIGURE 2. Diagram of the building model process.

TABLE 1. Lift factor parameters for different temperatures [34].

T	L_0	k	B_{c0}	b
30	6.12	0.07	3.23	1.41
40	5.29	0.10	1.86	1.12
50	4.12	0.17	1.26	0.96
65	2.44	0.61	0.59	0.77

vacuum permeability ($\mu_0 = 4\pi \times 10^{-7}\,\mathrm{H\,m^{-1}}$), taking into account that the resistivity of the superconducting material is several orders of magnitude lower than the resistivity of other materials forming the tape.

In this article, we consider a critical current density of $3\,\mathrm{MA\,cm^{-2}}$ at 77 K and an average temperature of 65 K. Since the tape's critical current density depends on temperature (T) and magnetic field ($\mathbf{B}$), we use a lift factor that models the anisotropic dependence on the local magnetic field [34]:

$$L = \frac{J_c(\mathbf{B}, T)}{J_c(77\,\mathrm{K})} = \frac{L_0(T)}{\left(1 + \frac{\sqrt{k(T)^2 B_\parallel^2 + B_\perp^2}}{B_{c0}(T)}\right)^{b(T)}} \tag{6}$$

In this equation, $J_c(\mathbf{B}, T)$ is the critical current density for a given temperature and magnetic field, L is the lift factor and the parameters: $L_0(T)$, $k(T)$, $B_{c0}(T)$ and $b(T)$ express the temperature dependence according to table 1 [34]. $B_\parallel$ and $B_\perp$ are the parallel and perpendicular (to the flat face of the tape) components of the magnetic flux density. We compute these parallel and perpendicular components by employing the dot product between the magnetic flux density and unitary vectors defining normal and tangential directions to each tape.

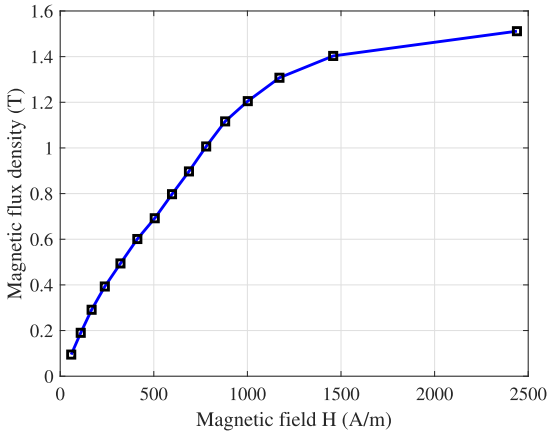

FIGURE 3. B-H curve of M330-50A at room temperature.

B. MAGNETIC MATERIAL

The magnetic material used in the design of the electrical machine is M330-50A. Measurements of the magnetic and electrical properties are presented in [32] and the relative permeability uploaded in the model is shown in Fig. 3. We assume that the magnetic material will be at room temperature, taking into account that only the superconductor is operating under cryogenic temperatures in the proposed designs.

C. MACHINE CROSS-SECTIONS AND MAIN PARAMETERS

The first machine design under study is based on distributed coils located in a stator with iron teeth. Each coil is assumed as a racetrack coil and four coil layers are stack one on top of the other inside a slot in one phase for one pole pair. These coils are connected in series. The whole machine

TABLE 2. Main parameters of the superconducting generator.

Number of slots	120
Number of pole pairs	20
Number of slots per pole pair	6
Remanent induction of permanent magnets	1.28 T
Number of coils per phase per pole pair	4
Number of turns per coil	50
Peak current in each coil	141.4 A
Nominal electrical frequency	3.33 Hz
Target nominal power	10 MW

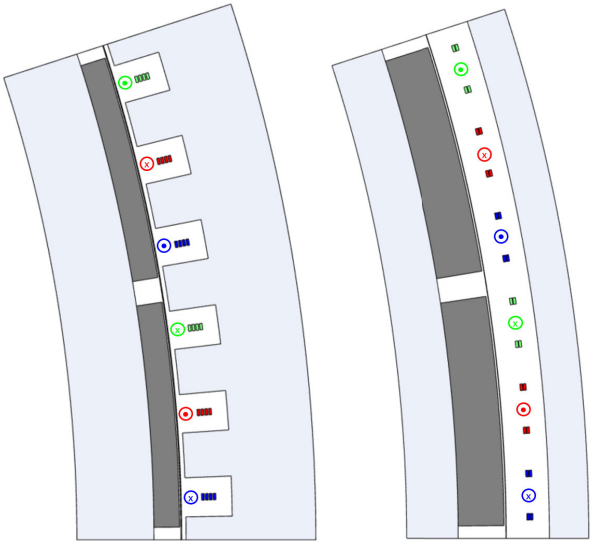

FIGURE 4. One pole pair cross-section of the first and second machine designs, from left to right: design with iron teeth and slotless design. Phase A is depicted in blue, B in red and C in green. The direction of the current is indicated in a circle close to the coils.

cross-section has 20 pole pairs and is designed with an effective length of 2.4 m to achieve a rated torque of 10 MN m. A summary of the characteristics of this machine is presented in table 2. The second design is very similar to the previous one. It uses the same coils, number of turns, number of pole pairs and magnets. However, the stator winding is designed as an airgap winding, so it has no teeth and is distributed with coils in two layers. This design has an effective length of 3.7 m to achieve a rated torque of 10 MN m. The geometry of one pole pair cross-section for both designs is presented in Fig. 4.

The third design is also similar to the first one, but the tape is assumed to be 2 mm wide instead of 4 mm. For this reason, each phase in one pole pair is composed of 8 coils stacked in groups of four. Each group of coils is separated inside the slot to decouple the magnetic field and reduce magnetization losses. The same lift factor and HTS parameters are used, but the tape's critical and transport current are reduced by half. The shape of the slot is modified to better guide the magnetic field from rotor to stator and to provide a low reluctance path for the self field to turn in the magnetic material and not so close to the stacks. This design has an effective length of 2.3 m to achieve the same rated torque. One pole pair cross-section of this design is shown in Fig. 5.

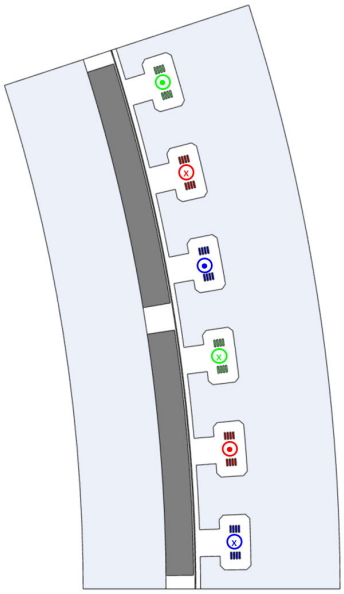

FIGURE 5. One pole pair cross-section of the third design. Phase A is depicted in blue, B in red and C in green. The direction of the current is indicated in a circle close to the coils.

IV. RESULTS AND LOSS ESTIMATION

In this section, estimation of losses and magnetic field behaviour are presented for the three machine designs. The resistive model approach is followed in each case to get the appropriated current distribution in the coils of the machine, which is then imported into the T-A formulation to compute losses in the HTS tapes.

A. BEHAVIOUR OF THE COILS OF EACH PHASE STUDIED WITH THE SUPERCONDUCTING MODEL

The main advantage of the superconducting model is that losses can be estimated and electromagnetic behaviour can be analyzed in each superconducting tape cross-section of the generator. Hence, this could be the first approach to study the superconducting machine. However, taking into consideration the aforementioned characteristics and geometry of one pole pair for the different designs, a similar electromagnetic behaviour (shifted in space and time) can be expected for the different coils of all the phases. To verify this hypothesis, we compare the normalized current density and magnetic field behaviour in the different coils cross-sections at different time instants. As it is shown in Fig. 6 for the first design, the current penetration and magnetic field behaviour is similar in the different phase coils cross-sections (rotated in space for the different phases) when the current in each one of them reaches its maximum and zero values (shifted in time for each phase).

The instantaneous losses can be computed in the n^{th} coil of phase A as:

$$P_{An}(\mathrm{W\,m^{-1}}) = \delta \int \mathbf{E} \cdot \mathbf{J} dl \tag{7}$$

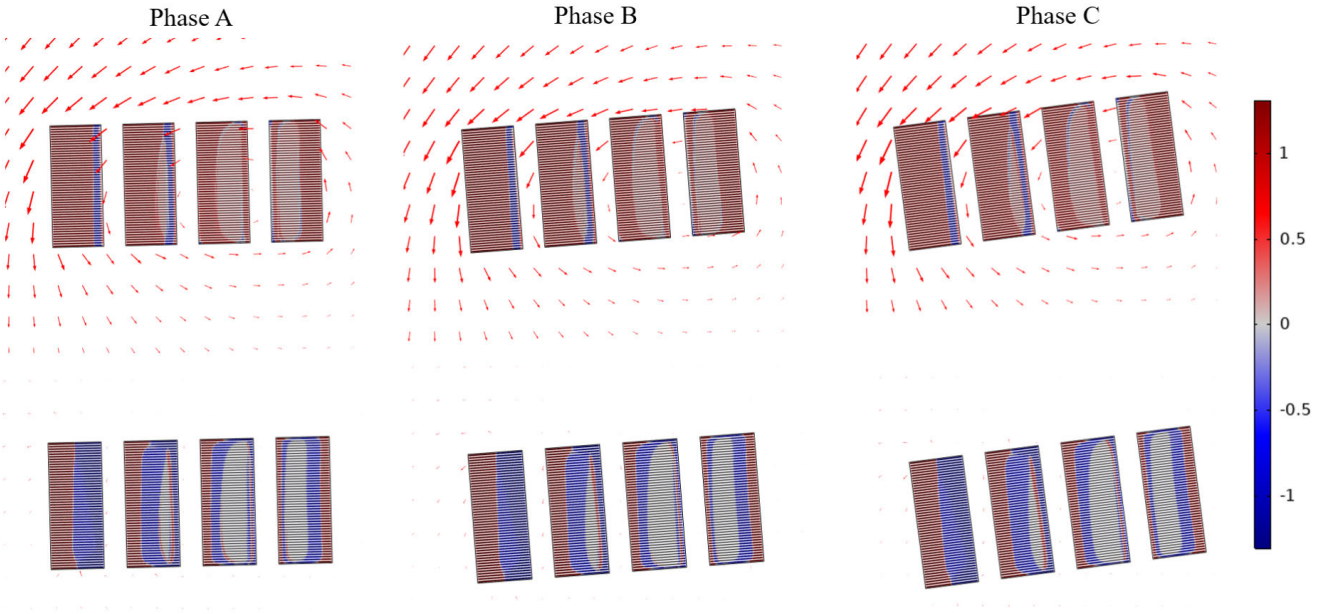

FIGURE 6. Behaviour of the normalized current density ($J/J_c(B)$) and magnetic field (red arrows) in the cross-section of each phase coil when the current of each phase is maximum (top) and zero (bottom) for the superconducting model of the first design.

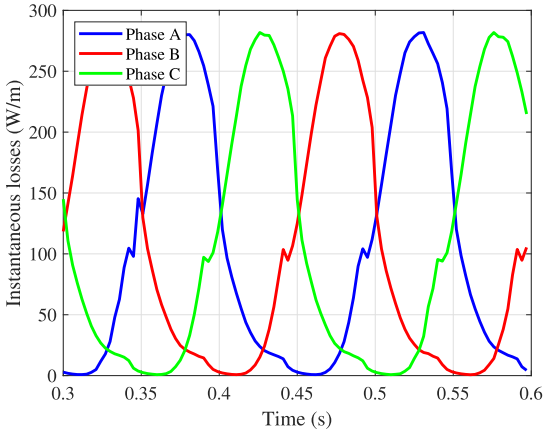

FIGURE 7. Instantaneous losses in the first racetrack coil, from left to right in Fig. 6, for each phase of the first design.

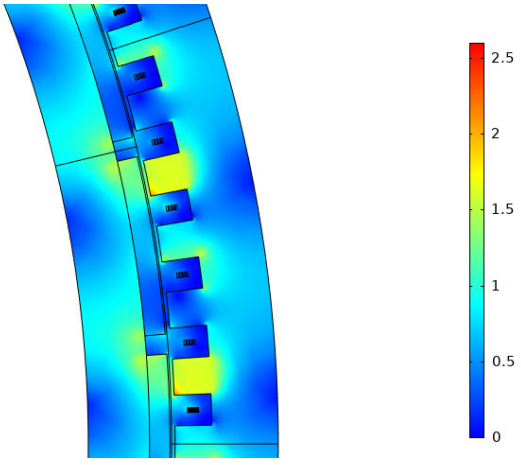

FIGURE 8. Magnetic flux density norm in T for one pole pair of the first design, when phase A current is maximum (time=0.375 s).

The losses computed with (7) in the first coil (from left to right) of Fig. 6 for the different phases are plotted in Fig. 7. As can be observed, they have the same periodic shape shifted in time. Losses in the rest of the coils behave in the same way, which can be expected given the above mentioned magnetic field and current density distribution.

From these results, we can say that the electromagnetic behaviour and losses can be analyzed with the same accuracy when the calculations of one phase coil group are extrapolated into the other phases. Therefore, we can model only one group of coils as superconducting material and homogenize all the other coils cross-sections. This allows us to keep the same general electromagnetic behaviour and reduce computation time.

B. DESIGN WITH IRON TEETH

The magnetic flux density norm in the cross-section of one pole pair for this first design is shown in Fig. 8 and the instantaneous losses are presented in Fig. 9. The windings are numbered from left to right. The coils with higher losses, located closer to the rotor, also experience a higher current penetration and a higher perpendicular magnetic field.

These results show a strong relationship between losses and magnetic field. For instance, if we analyze only the self field (Fig. 10) and consider the interaction between two coils, the perpendicular (to the flat face of the tape) magnetic field between the coils is reduced, since both carry the same current. However, when we consider 3 or more coils, the perpendicular magnetic field increase in the first

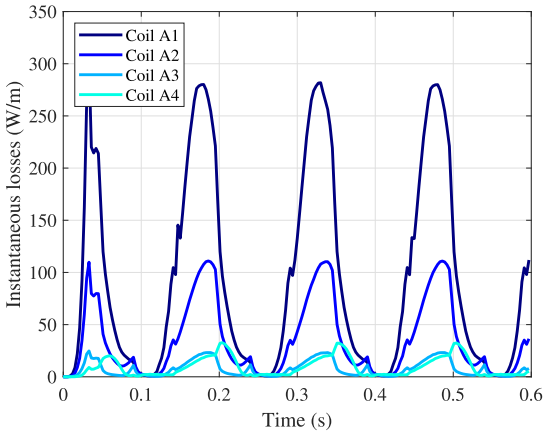

FIGURE 9. Losses in the coils of phase A for the first design, in Fig. 4 the first coils from bottom to top numbered from left to right as A1, A2, A3 and A4.

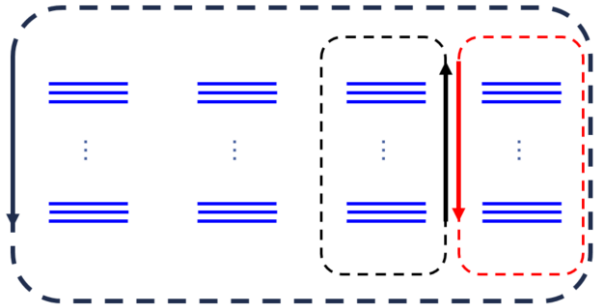

FIGURE 10. Basic schematic behaviour of the self field in the coils cross-section for the first design.

and last windings of the array. The magnetic field norm can further increase in the first ones since these are closer to the rotor. However, the last ones are closer to stator iron and partially shielded by coils 1 and 2. This causes a lower magnetic field around the last coils, where we have lower losses.

To estimate the losses, we analyze only the second period of the sinusoidal cycle. The first half cycle includes a transient behaviour that does not represent the AC operating regime of the HTS tapes. The overall behaviour of the losses can be better appreciated in Fig. 11, where the average power dissipation in the cross-section of phase A coil group is shown. This power density is calculated in each point of the tapes as:

$$\frac{1}{T}\int_{T}^{2T} \mathbf{E}\cdot\mathbf{J}dt \tag{8}$$

In this figure, we can observe that coil 1 has the highest average dissipation. Hence it could be under higher thermal stress. To calculate the losses in phase A coil group, we can integrate the dissipation in all the coils of this phase:

$$Q_A(\mathrm{J\,m^{-1}}) = \int_{T}^{2T}\sum_{n=1}^{4}(P_{An})dt \tag{9}$$

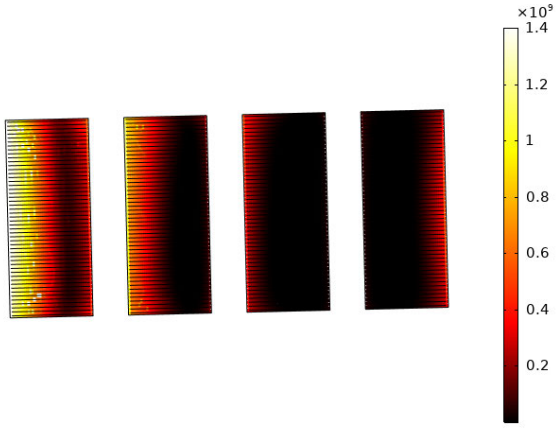

FIGURE 11. Average power density dissipation (W $\mathrm{m^{-3}}$) of the phase A coil group for the first design.

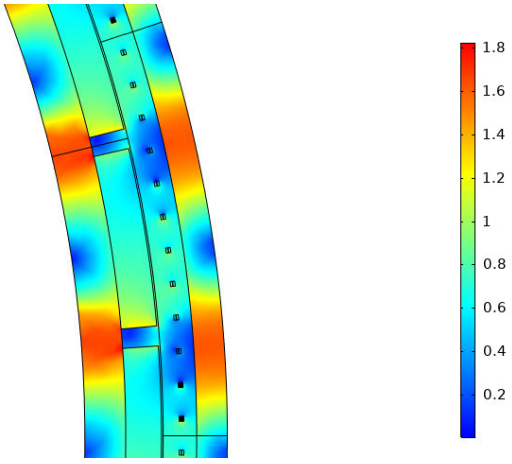

FIGURE 12. Magnetic flux density norm in T for one pole pair of the second design, when phase A current is maximum (time=0.375 s).

The total losses in the superconducting windings can be obtained by multiplying the result of (9) by the number of coil groups (6), the number of pole pairs (20), active length of the machine (2.4 m) and nominal frequency (3.33 Hz). This results in a total loss of 46.85 kW.

C. SLOTLESS DESIGN

The model for the second design is built by following a similar approach. The superconducting model yields the same behaviour per coil group in this design too. Therefore, we focus on the first four coils cross-section (from bottom to top), depicted in blue in Fig. 4.

The magnetic flux density norm in the cross-section of one pole pair is shown in Fig. 12 and the instantaneous losses in the four coils cross-section are presented in Fig. 13. The coils have been numbered from left (closer to rotor) to right (closer to stator) and from bottom to top.

In this design, the current penetration in all the four coils cross-section is more uniform, as it is shown in Fig. 14. Moreover, the average power density dissipation (Fig. 15) is better

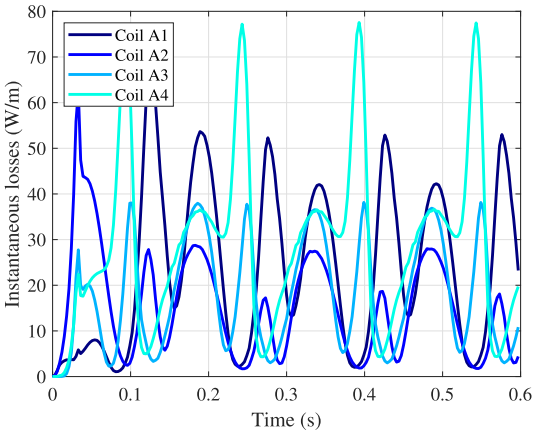

FIGURE 13. Losses in the coils of phase A for the second design, in Fig. 4 the first coils at the bottom numbered from left to right and bottom to top, as A1, A2, A3 and A4.

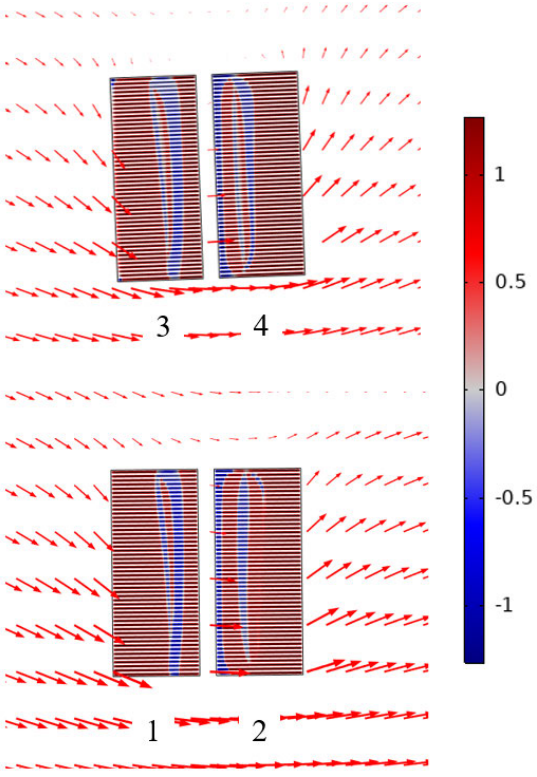

FIGURE 14. Behaviour of the normalized current density ($J/J_c(\mathbf{B})$) and magnetic field (red arrows) in the cross-section of the coils of phase A for the second design, when the current in the coil group is maximum.

distributed. Only coil number four experiences slightly higher losses compared to the others. This behaviour supports the aforementioned analysis regarding the interaction between only two coils.

To calculate losses in phase A coil group, we can integrate again the dissipation by using (9). The total losses in all the coils of the machine can be obtained if we multiply by the number of coil groups (6), the number of pole pairs (20), active length of the machine (3.7 m) and nominal frequency (3.33 Hz). This results in a total loss of 39.81 kW.

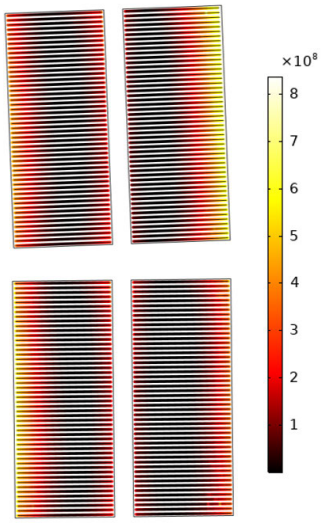

FIGURE 15. Average power density dissipation (W m^{-3}) of the phase A coil group for the second design, in Fig. 4 the first coils from bottom to top in blue.

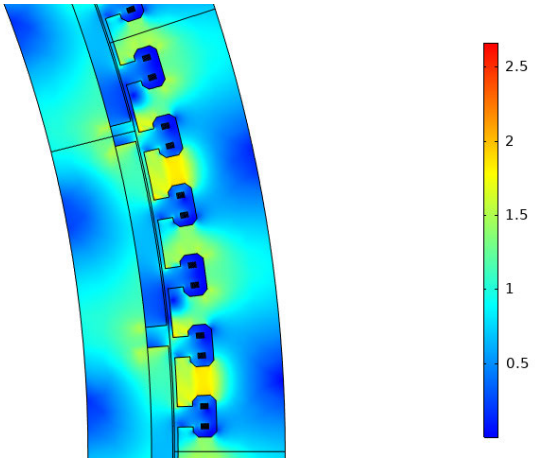

FIGURE 16. Magnetic flux density norm in T for one pole pair of the third design, when phase A current is maximum.

D. DESIGN WITH IMPROVEMENTS IN SLOT SHAPE AND COILS POSITION

In this section, we change the superconducting tape in the first design from 4 mm to 2 mm wide to reduce losses. The same parameters are used and the transport and critical current are reduced to half. Initially, the number of coils is increased from 4 to 8, stacked in the same position and connected in series. A similar electromagnetic behaviour was obtained, with roughly 44 % reduction in the losses of the HTS coils (total in coils, 26.11 kW), in comparison with the first design. However, the coils closer to the rotor still experience a much higher energy dissipation.

In order to reduce the effect mentioned in Fig. 10, we separate the 8 coils inside a slot, as can be observed in Fig. 5. An angular separation was kept between both sub-groups of four coils. This introduces a high reluctance that can decouple the magnetic field. Moreover, the shape of the slot was modified by trimming the corners, in order to provide a better path

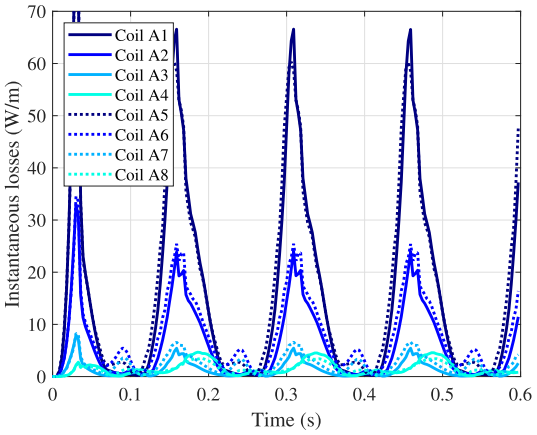

FIGURE 17. Losses in the 8 coils of phase A for the third design. In Fig. 5 the first coils at the bottom, numbered from left to right and from bottom to top.

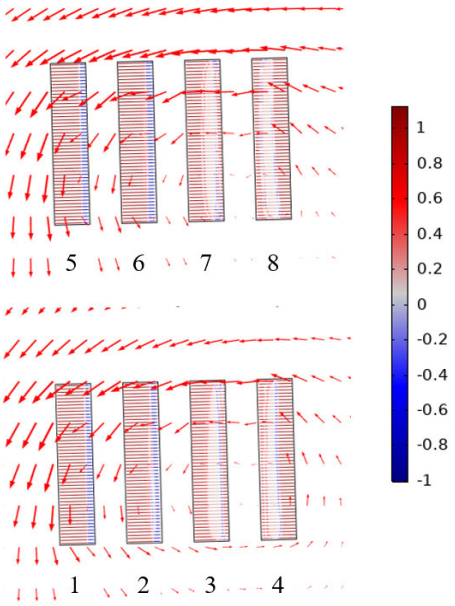

FIGURE 18. Behaviour of the normalized current density ($J/J_c(\mathbf{B})$) and magnetic field (red arrows) in the cross-section of the coils of phase A for the third design, when the current in the coil group is maximum (both coils sub-groups are printed closer for a better comparison).

for the magnetic field to turn in the magnetic material. The coils were also put a bit deeper in the stator and the area of the stator iron closer to the rotor was increased to guide better the magnetic field from rotor to stator.

The same modelling methodology was repeated for this new design. The magnetic flux density norm in the cross-section of one pole pair can be observed in Fig. 16. The Instantaneous losses in the eight coils cross-section are shown in Fig. 17, where the coils have been numbered from left (closer to rotor) to right (closer to stator) and from bottom to top. As can be appreciated, the losses of the different sub-groups are very similar.

In this design, the current penetration is also similar between sub-groups, as can be observed in Fig. 18. Moreover, a good distribution of the average power density dissipation

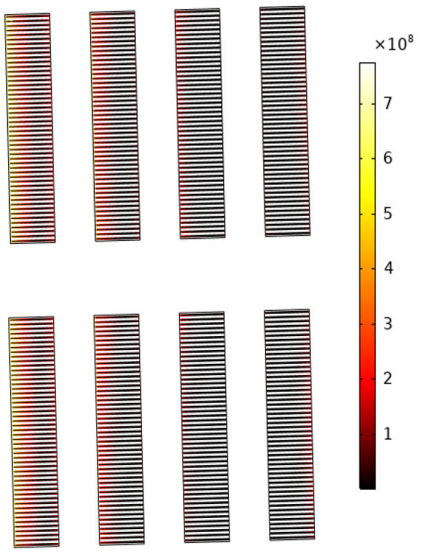

FIGURE 19. Average power density dissipation (W m^{-3}) of the phase A coil group for the third design (both coils sub-groups are printed closer for a better comparison).

is achieved (Fig. 19), in comparison with the first design. However, coils number one and five still experience higher dissipation in comparison to the other coils in the group. This behaviour could be related to the horizontal array and the magnetic field contribution coming from the rotor.

Losses in the superconducting coils are estimated by following the same procedure. In this design, the total loss in the coils is 15.73 kW. This means approximately a 40 % additional reduction. However, the positions of the coils inside a slot followed only a heuristic approach which aimed at verifying the impact of the magnetic field behaviour in the losses. Since it brought a high reduction in losses and a better distribution of the average power density dissipation, a formal optimization process can be done by considering the angular separation of the coils sub-groups (to decouple the magnetic field between the coils) and the radial location of the coils. The objective could be to minimize the losses in the HTS material (increasing the efficiency of the machine) and to maximize the torque density (decreasing machine length, materials and price). This multi-objective optimization process is proposed as future work and it can be carried out with one resistive and one HTS coil model by updating the current distribution, calculating torque density and losses on every step.

E. BEHAVIOUR OF THE LOSSES FOR DIFFERENT FREQUENCIES AND TEMPERATURES

All the results presented so far considered a temperature of 65 K and a frequency of 3.33 Hz. To verify the impact of these variables in HTS losses, we performed a sensitivity analysis by repeating computations in a parametric study for the three designs. The performance for different frequencies and an average temperature of 65 K is presented in Fig. 20.

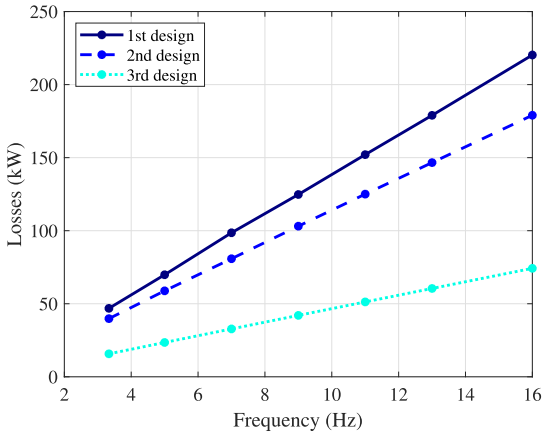

FIGURE 20. Behaviour of the losses in each design for different frequencies and an average temperature of 65 K.

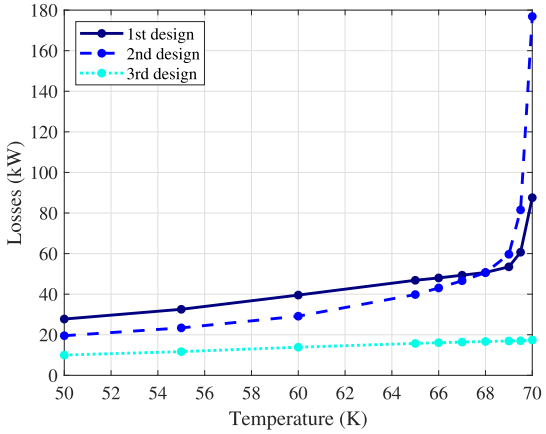

FIGURE 21. Behaviour of the losses in each design for different temperatures and a frequency of 3.33 Hz.

This figure shows a linear increase in the losses in kW with the frequency. This linear nature reflects a similar electromagnetic behaviour per cycle, repeated at different speeds for different frequencies.

The performance for different temperatures and a nominal frequency of 3.33 Hz is presented in Fig. 21. This figure shows a big increase in the losses in the first and second design when the average temperature increase over 68 K. This behaviour is probably related to current saturation in the coils and the non-linear dependence of the critical current density on the magnetic field and temperature. Losses in the third design have a more steady behaviour. This means a safer operation of the coils in case of transient increase of temperature and it could allow us to operate normally at temperatures higher than 65 K, where higher cooling efficiencies can be achieved.

V. CONCLUSION

The electromagnetic behaviour of synchronous superconducting machines was analyzed. The T-A formulation was used and the current distribution was addressed by following a proposed methodology based on the building model process. This allows us to improve superconducting machine

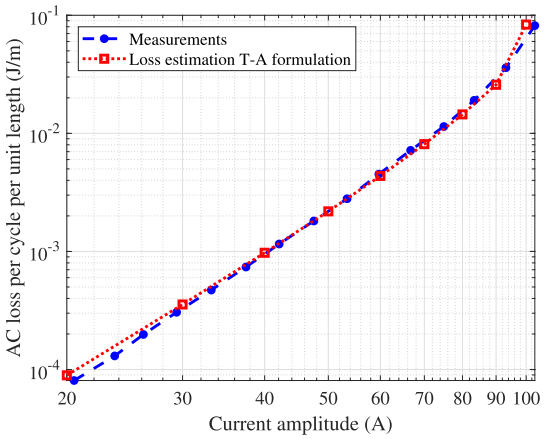

FIGURE 22. Comparison of the losses estimated with the T-A formulation and measurements for a circular coil [28].

designs by reducing the losses in superconducting coils with a detailed analysis.

The modelling approach was implemented on a 10 MW generator with permanent magnets in the rotor and superconducting coils in the stator. Three solutions were considered. First, a design with iron teeth and four coil layers per slot was analyzed. Then, a slotless solution was modelled and a small reduction in losses was achieved. Based on these two results, a new design was proposed. In this last solution, the electromagnetic behaviour and losses in the machine were improved by changing the shape of the slot, location of the coils and width of the HTS tape. We show with this design study implementation that the proposed methodology can address the design of the machine and the estimation of losses in the HTS tapes with a single building model process. Moreover, a design optimization was proposed as future work to increase machine efficiency (minimizing losses in the HTS coils) and reduce cost (reducing the length of the machine) based on this modelling approach.

Finally, a sensitivity analysis was conducted over the nominal frequency of the machine and the average temperature of the coils. This study shows a linear increase of losses in kW with the frequency under constant temperature. The first and second designs experience a large increase of losses with temperatures higher than 68 K. The third design has a more steady behaviour of the losses in case of disturbances in temperature. These results are useful for the design of the cooling system and provide guidance for coils operation and future applications.

APPENDIX

The T-A formulation has been used in this article as a modelling technique for superconducting coils. To validate this approach against measurements, we estimated losses in the coil presented in [28]. This is a circular coil with an internal diameter of 60 mm and an external diameter of 67.8 mm, made with 24 turns of a 4 mm tape. It was modelled as an axisymmetric problem and we considered a critical electric field E_c of 1×10^{-4} V m^{-1} and a value of $n = 25$. Further

information about the coil, tape and measurement technique can be found on [28], [35].

Losses were estimated for a sinusoidal transport current with a frequency of 36 Hz without an external magnetic field. The amplitude of the current was changed in a parametric study from 20 A to 100 A. Fig. 22 shows a comparison of the losses estimated with the T-A formulation and measurements conducted in [28]. As can be observed, the model is in good agreement with the measurements.

ACKNOWLEDGMENT

The authors thank Dr.-Ing. Yingzhen Liu for providing measurements of the permeability of the magnetic material at room temperature and sharing expertise in machine designs.

REFERENCES

[1] S. S. Kalsi, *Applications of High Temperature Superconductors to Electric Power Equipment*. Hoboken, NJ, USA: Wiley, Mar. 2011. [Online]. Available: http://doi.wiley.com/10.1002/9780470877890

[2] M. Zhang, M. Chudy, W. Wang, Y. Chen, Z. Huang, Z. Zhong, W. Yuan, J. Kvitkovic, S. V. Pamidi, and T. A. Coombs, "AC loss estimation of HTS armature windings for electric machines," *IEEE Trans. Appl. Supercond.*, vol. 23, no. 3, Jun. 2013, Art. no. 5900604.

[3] K. S. Haran, S. Kalsi, T. Arndt, H. Karmaker, R. Badcock, B. Buckley, T. Haugan, M. Izumi, D. Loder, J. W. Bray, P. Masson, and E. W. Stautner, "High power density superconducting rotating machines—Development status and technology roadmap," *Superconductor Sci. Technol.*, vol. 30, no. 12, Nov. 2017, Art. no. 123002.

[4] C. C. Rong and P. N. Barnes, "Developmental challenges of SMES technology for applications," *IOP Conf. Ser., Mater. Sci. Eng.*, vol. 279, Dec. 2017, Art. no. 012013.

[5] W. H. Fietz, M. J. Wolf, A. Preuss, R. Heller, and K.-P. Weiss, "High-current HTS cables: Status and actual development," *IEEE Trans. Appl. Supercond.*, vol. 26, no. 4, Jun. 2016, Art. no. 4800705.

[6] I. K. Okakwu, P. E. Orukpe, and E. A. Ogujor, "Application of superconducting fault current limiter (SFCL) in power systems: A review," *Eur. J. Eng. Res. Sci.*, vol. 3, no. 7, pp. 28–32, Jul. 2018.

[7] S. S. Kalsi, "Superconducting wind turbine generator employing MgB_2 windings both on rotor and stator," *IEEE Trans. Appl. Supercond.*, vol. 24, no. 1, Feb. 2014, Art. no. 5201907.

[8] G. Snitchler, B. Gamble, C. King, and P. Winn, "10 MW class superconductor wind turbine generators," *IEEE Trans. Appl. Supercond.*, vol. 21, no. 3, pp. 1089–1092, Jun. 2011.

[9] J. Lloberas, A. Sumper, M. Sanmarti, and X. Granados, "A review of high temperature superconductors for offshore wind power synchronous generators," *Renew. Sustain. Energy Rev.*, vol. 38, pp. 404–414, Oct. 2014.

[10] B. B. Jensen, N. Mijatovic, and A. B. Abrahamsen, "Development of superconducting wind turbine generators," *J. Renew. Sustain. Energy*, vol. 5, no. 2, Mar. 2013, Art. no. 023137.

[11] I. Marino, A. Pujana, G. Sarmiento, S. Sanz, J. M. Merino, M. Tropeano, J. Sun, and T. Canosa, "Lightweight MgB_2 superconducting 10 MW wind generator," *Superconductor Sci. Technol.*, vol. 29, no. 2, Dec. 2015, Art. no. 024005.

[12] R. Wesche, *Physical Properties of High-Temperature Superconductors*. London, U.K.: Wiley, 2015.

[13] M. P. Oomen, J. Rieger, V. Hussennether, and M. Leghissa, "AC loss in high-temperature superconducting conductors, cables and windings for power devices," *Superconductor Sci. Technol.*, vol. 17, no. 5, pp. S394–S399, Apr. 2004.

[14] W. T. Norris, "Calculation of hysteresis losses in hard superconductors carrying AC: Isolated conductors and edges of thin sheets," *J. Phys. D, Appl. Phys.*, vol. 3, no. 4, pp. 489–507, Apr. 1970.

[15] E. H. Brandt and M. Indenbom, "Type-II-superconductor strip with current in a perpendicular magnetic field," *Phys. Rev. B, Condens. Matter*, vol. 48, no. 17, pp. 12893–12906, Nov. 1993.

[16] Y. Mawatari, "Critical state of periodically arranged superconducting-strip lines in perpendicular fields," *Phys. Rev. B, Condens. Matter*, vol. 54, no. 18, pp. 13215–13221, Nov. 1996.

[17] Y. Mawatari, "Critical state in superconducting strip-array systems with transport current," in *Advances in Superconductivity IX*. Japan: Springer-Verlag, Oct. 1997, pp. 575–580.

[18] G. P. Mikitik, Y. Mawatari, A. T. S. Wan, and F. Sirois, "Analytical methods and formulas for modeling high temperature superconductors," *IEEE Trans. Appl. Supercond.*, vol. 23, no. 2, Apr. 2013, Art. no. 8001920.

[19] T. Benkel, M. Lao, Y. Liu, E. Pardo, S. Wolfstädter, T. Reis, and F. Grilli, "T–A-formulation to model electrical machines with HTS coated conductor coils," *IEEE Trans. Appl. Supercond.*, vol. 30, no. 6, Sep. 2020, Art. no. 5205807.

[20] X. Huang, Z. Huang, X. Xu, L. Wang, W. Li, and Z. Jin, "A fully coupled numerical method for coated conductor HTS coils in HTS generators," *IEEE Trans. Appl. Supercond.*, vol. 30, no. 4, Jun. 2020, Art. no. 5206406.

[21] Y. Yang, H. Yong, X. Zhang, and Y. Zhou, "Numerical simulation of superconducting generator based on the T–A formulation," *IEEE Trans. Appl. Supercond.*, vol. 30, no. 8, Dec. 2020, Art. no. 5207611.

[22] Y. Gao, W. Wang, X. Wang, H. Ye, Y. Zhang, Y. Zeng, Z. Huang, Q. Zhou, X. Liu, Y. Zhu, and Y. Lei, "Design, fabrication, and testing of a YBCO racetrack coil for an HTS synchronous motor with HTS flux pump," *IEEE Trans. Appl. Supercond.*, vol. 30, no. 4, Jun. 2020, Art. no. 4601005.

[23] H. Zhang, M. Zhang, and W. Yuan, "An efficient 3D finite element method model based on the T–A formulation for superconducting coated conductors," *Superconductor Sci. Technol.*, vol. 30, no. 2, Dec. 2016, Art. no. 024005.

[24] F. Liang, S. Venuturumilli, H. Zhang, M. Zhang, J. Kvitkovic, S. Pamidi, Y. Wang, and W. Yuan, "A finite element model for simulating second generation high temperature superconducting coils/stacks with large number of turns," *J. Appl. Phys.*, vol. 122, no. 4, Jul. 2017, Art. no. 043903.

[25] E. Berrospe-Juarez, V. M. R. Zermeño, F. Trillaud, and F. Grilli, "Real-time simulation of large-scale HTS systems: Multi-scale and homogeneous models using the T–A formulation," *Superconductor Sci. Technol.*, vol. 32, no. 6, Apr. 2019, Art. no. 065003.

[26] E. Berrospe-Juarez, V. M. R. Zermeno, F. Trillaud, A. Gavrilin, F. Grilli, D. V. Abraimov, D. K. Hilton, and H. W. Weijers, "Estimation of losses in the (RE)BCO two-coil insert of the NHMFL 32 T all-superconducting magnet," *IEEE Trans. Appl. Supercond.*, vol. 28, no. 3, Apr. 2018, Art. no. 4602005.

[27] J. Rhyner, "Magnetic properties and AC-losses of superconductors with power law current—Voltage characteristics," *Phys. C, Supercond.*, vol. 212, nos. 3–4, pp. 292–300, Jul. 1993.

[28] E. Pardo, J. Šouc, and L. Frolek, "Electromagnetic modelling of superconductors with a smooth current–voltage relation: Variational principle and coils from a few turns to large magnets," *Superconductor Sci. Technol.*, vol. 28, no. 4, Feb. 2015, Art. no. 044003.

[29] A. Fatemi, D. M. Ionel, N. A. O. Demerdash, D. A. Staton, R. Wrobel, and Y. C. Chong, "A computationally efficient method for calculation of strand eddy current losses in electric machines," in *Proc. IEEE Energy Convers. Congr. Expo. (ECCE)*, Sep. 2016, pp. 1–8.

[30] F. Chauvicourt, P. Romanazzi, D. Howey, A. Dziechciarz, C. Martis, and C. T. Faria, "Review of multidisciplinary homogenization techniques applied to electric machines," in *Proc. 11th Int. Conf. Ecol. Vehicles Renew. Energies (EVER)*, Apr. 2016, p. 9.

[31] P. Nirmal. *How to Analyze an Induction Motor: A TEAM Benchmark Model*. Accessed: Aug. 15, 2020. [Online]. Available: https://www.comsol.jp/blogs/how-to-analyze-an-induction-motor-a-team-benchmark-model/

[32] Y. Liu, M. Noe, J. Ou, P. Breining, M. Veigel, and M. Doppelbauer, "Measurement of magnetic materials at room and cryogenic temperature for their application to superconducting wind generators," *IEEE Trans. Appl. Supercond.*, vol. 28, no. 3, Apr. 2018, Art. no. 5206006.

[33] D. Hazelton. (Apr. 2013). *Status of 2G HTS Wire for Electric Power Applications*. [Online]. Available: http://www.superpower-inc.com/system/files/2013_0426+CIGRE+WG38+Wksp_SuperPower.pdf

[34] S. Zou, V. M. R. Zermeno, and F. Grilli, "Simulation of stacks of high-temperature superconducting coated conductors magnetized by pulsed field magnetization using controlled magnetic density distribution coils," *IEEE Trans. Appl. Supercond.*, vol. 26, no. 3, Apr. 2016, Art. no. 8200705.

[35] E. Pardo, J. Šouc, and J. Kováč, "AC loss in ReBCO pancake coils and stacks of them: Modelling and measurement," *Superconductor Sci. Technol.*, vol. 25, no. 3, Jan. 2012, Art. no. 035003.

CARLOS ROBERTO VARGAS-LLANOS received the B.Eng. degree (Hons.) in electrical engineering from the University of Carabobo, Carabobo, Venezuela, in 2011, and the M.Eng. degree in electrical engineering from the Universidad Nacional Autónoma de México, México City, México, in 2015. He is currently pursuing the Ph.D. degree in electrical engineering with the Karlsruhe Institute of Technology, Karlsruhe, Germany.

From 2015 to 2016, he was a Design Engineer with Industrias IEM, México. From 2016 to 2019, he was a Supervisor with the National Center for Energy Control (CENACE), Planning Department, México City. His main research interests include superconducting electrical machines, two-dimensional and three-dimensional modeling of high-temperature superconductors, renewable energies, electric power systems transient, and stability behaviour.

SEBASTIAN LENGSFELD was born in Hanover, Germany, in 1992. He received the M.Sc. degree in mechatronics from the Leibniz University of Hanover, in 2019.

He has been with the Fraunhofer Institute for Energy Economics and Energy System Technology, Kassel, since 2019. His research interest includes electromechanical machine designs in wind power applications.

FRANCESCO GRILLI received the M.S. degree in physics from the University of Genoa, Italy, in 1998, the Ph.D. degree in technical sciences from the École Polytechnique Fédérale de Lausanne, Switzerland, in 2004, and the Habilitation degree in superconductivity for energy applications from the Karlsruhe Institute of Technology, Germany, in 2017.

From 2004 to 2007, he was a Postdoctoral Researcher with the Los Alamos National Laboratory, USA. From 2007 to 2009, he was with the Polytechnique Montréal, Montréal, QC, Canada. Since 2009, he has been with the Karlsruhe Institute of Technology, Germany, where he is currently the Leader of the Group AC Losses in High-Temperature Superconductors. His main research interests include 2-D and 3-D modeling of high-temperature superconductors and dc and ac characterization of their properties.

Dr. Grilli was a recipient of the 2008 and 2014 Van Duzer Prize for the Best Contributed Non-Conference Paper published in the IEEE TRANSACTIONS ON APPLIED SUPERCONDUCTIVITY and the 2011 Dr. Meyer-Struckmann Science Prize for the work on numerical modeling of superconductors.